Acceleration Estimator for Low-Velocity and Low-Acceleration Regions Based on Encoder Position Data

Se-Han Lee and Jae-Bok Song

***Abstract*—Acceleration computation based on simple numerical differentiation from an optical encoder signal may be very erroneous, especially in the low-velocity and low-acceleration regions. To overcome this problem, a novel approach to estimating acceleration in these regions is proposed in this paper. This so-called low-acceleration estimator, which is a computer algorithm, is based on the fact that the displacement signal from the encoder is accurate. Since the bandwidth of this estimator is rather limited, it can be used in combination with the traditional numerical differentiation approach in order to cover a wide velocity range. It was shown in various simulations and experiments that this combined acceleration estimator can yield accurate acceleration estimates over a wide range of velocities. Furthermore, when this estimator is applied to a friction compensation system, the effect of low-velocity friction can be reduced significantly by its capability to detect small changes in acceleration caused by friction.**

***Index Terms*—Low-acceleration estimator, low-acceleration region, low-velocity region, M/T method.**

I. Introduction

THE precision of mechanical systems using servo motors has been greatly improved thanks to advancement of position and velocity control techniques. Optical encoders are widely used for both position and velocity measurements in most applications associated with the servo motors due to high resolution, high accuracy, and relative ease of adaptation in digital control systems [1].

Velocity sensing based on an optical encoder is usually done by either a fixed-time or fixed-position method. A fixed-time method, also called a pulse-counting or "M" method, estimates the velocity by counting the pulses over a fixed sampling period. A fixed-position method, also called a pulse-timing or "T" method, estimates the velocity by measuring the time for one encoder pulse using a high-frequency auxiliary clock signal. It is well known, however, that the fixed-time and fixed-position methods are inaccurate at low and high velocity ranges, respectively. Therefore, Ohmae [2] proposed a so-called M/T method, which generates accurate velocities over a wide range of velocities by combining these two methods. One drawback of the M/T method is that the detection period is always variable. For example, the detection period becomes very lengthy in the low-velocity region, and thus only average velocity can be obtained instead of instantaneous velocity. On the other hand, acceleration is usually computed by numerical differentiation (ND), in which the difference between successive velocities is divided by the time interval, but the numerical differentiation inherently generates inaccurate results, particularly in the low-velocity and/or low-acceleration regions. In addition, the differentiation process tends to magnify errors or noises.

Some research has been done to improve accuracy of velocity and acceleration sensing from the optical encoder signals. Some researchers employed a Kalman filter to estimate the velocity and/or acceleration accurately [3], [4]. Since this approach requires the target velocity and acceleration trajectories, which should be sent to the filter, it cannot be applied to the case where arbitrary velocity and acceleration are measured. Dunworth [5] used some hardware to detect the frequency of the encoder signal, but this method requires a rather long sampling period inadequate for high-speed applications. Nicosia [6] used a nonlinear observer to obtain the angular velocities, but its applications are limited since the observer requires the complete nonlinear model.

In this paper, a new algorithm for acceleration estimation is proposed. This so-called low-acceleration estimator (LAE) is based on two facts: the displacement information based on the encoder signal is very accurate and numerical integration is more stable and accurate than numerical differentiation. This approach has some advantages over other approaches. First, this estimator does not require system models needed for a Kalman filter or other observer-based approaches. Second, accurate acceleration estimation can be achieved even in very low velocity and/or very low acceleration ranges, in which acceleration sensing is usually very difficult.

This paper presents some difficulties in sensing acceleration in the low-velocity and low-acceleration ranges both analytically and experimentally. Then the features and performance of the proposed low-acceleration estimator are discussed in detail. Finally, the proposed acceleration estimator will be applied to friction compensation control systems in order to verify its validity.

II. Acceleration Estimation Based on Numerical Differentiation

A. Experimental Setup

Fig. 1 shows the experimental setup used in observing performance of acceleration computation done by an acceleration estimator proposed in this research. The servo system is made up of a three-phase and four-pole brushless dc (BLDC) linear motor equipped with an optical encoder with a resolution of 0.5 μm/pulse. A linear motor has the same operating principle as a rotary motor, except that the former consists of moving

Manuscript received January 17, 2000; revised October 10, 2000. Recommended by Technical Editor K. Ohnishi.

The authors are with the Department of Mechanical Engineering, Korea University, Seoul 136-701, Korea (e-mail: jbsong@korea.ac.kr).

Publisher Item Identifier S 1083-4435(01)02717-X.

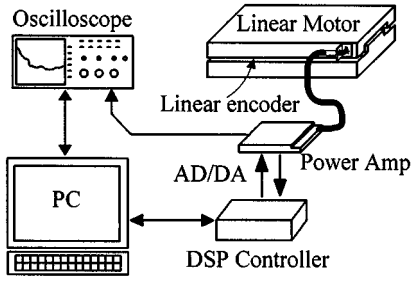

Fig. 1. Schematic of experimental setup.

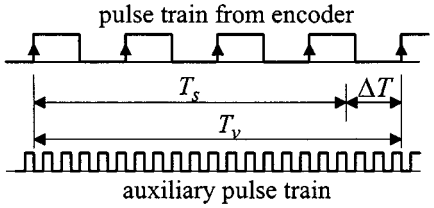

Fig. 2. Timing diagram of velocity measurement using M/T method.

and stationary parts corresponding to the rotor and stator of the latter. The control logic for driving a motor is realized using the TMS320C31 DSP board and the voltage-driven pulse-width modulation (PWM) power amplifier.

The sampling period T_s of this system is set to 400 μs, since the PWM power amplifier has a bandwidth of 2.5 kHz. Further reduction in T_s may degrade the accuracy of velocity measurement, especially in the low-velocity region. The period of auxiliary clock pulses Δt used to measure the additional time ΔT is set to 1 μs.

B. Velocity Measurement by M/T Method

As shown in Fig. 2, the period T_v used for an M/T method is composed of the sampling period T_s and the additional time ΔT required for the encoder pulse to become an integer multiple. That is, T_v spans from the rising edge of the encoder pulse to the first rising edge after T_s has elapsed. The displacement x and velocity v during T_v are then obtained by

$$x = mR \tag{1}$$

$$v = \frac{x}{T_v} = \frac{mR}{T_s + \Delta T} \tag{2}$$

where m is the number of the encoder pulses and R (μm/pulse) is the encoder resolution.

Let us consider the velocity detection at low velocity based on the M/T method. Fig. 3 shows the simulation results in which the direction of a linear motor changes and passes the zero velocity point. The number of pulses m gradually drops as the velocity decreases, and then increases after passing the zero velocity with the negative sign. On the other hand, it is observed that the additional time ΔT, while very small at most velocity ranges, sharply increases in the low-velocity region marked by a circle. For example, no pulse appears near the zero velocity region, and thus ΔT required for the next rising edge becomes significantly large. In Fig. 3, where $T_s = 400$ μs is assumed, $\Delta T = 2\,600$ μs is needed for velocity computation based on the M/T method, thus leading to $T_v = 3000$ μs. This corresponds to about 7.5 times the sampling period, and an update of velocity information (and acceleration as well) is unavailable during this interval. Such a low

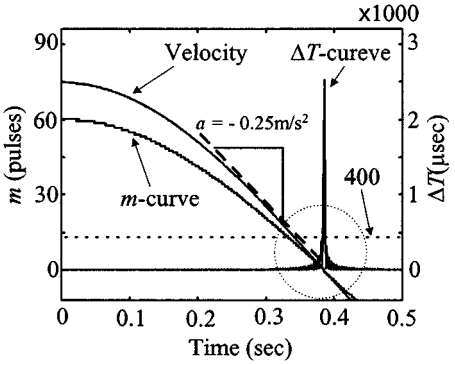

Fig. 3. Number of encoder pulses m and auxiliary period ΔT at low velocity (simulation).

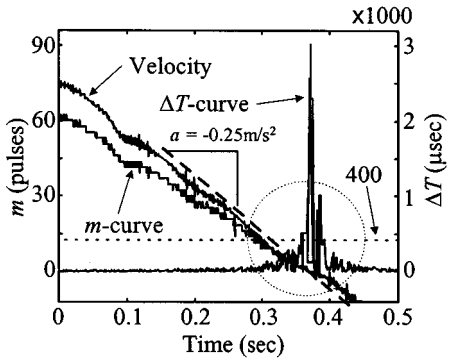

Fig. 4. Number of encoder pulses m and auxiliary period ΔT at low velocity (experiment).

(or zero) velocity region, usually caused by direction change, is inevitable in real servo control problems. Fig. 4 shows the experimental result for the same situation as in Fig. 3. The tendency of a sharp increase in ΔT near the zero velocity region is similar to the simulation, but a discontinuity in ΔT appears in the experimental result. This is because the motor repeats the stick-and-slip phenomenon due to frictional force.

In summary, the velocity using an M/T method is accurate over a wide range of velocities, but a drawback is that only the average velocity taken during a long period can be determined around the low-velocity region.

C. Acceleration Estimation by Numerical Differentiation

Acceleration based on an optical encoder is generally obtained by numerically differentiating the velocity computed based on an M/T method. Although the accuracy of this approach is acceptable over a wide velocity region, it is likely that the acceleration will become very inaccurate around the low-acceleration and/or low-velocity regions. In what follows, the analytical investigation of this problem is considered. First, the acceleration computation near the zero acceleration region will be examined.

Suppose that the linear motor performs a motion with a sinusoidal velocity profile

$$v_r = V\cos(\omega t) \tag{3}$$

where v_r represents the desired reference velocity, which may be slightly different from the actual velocity, and V and ω denote the amplitude (assumed to be 0.04 m/s in the simulation) and frequency, respectively. Though a sinusoidal velocity profile is assumed for convenience, the result of this analysis can be readily extended to arbitrary velocity profiles. Furthermore,

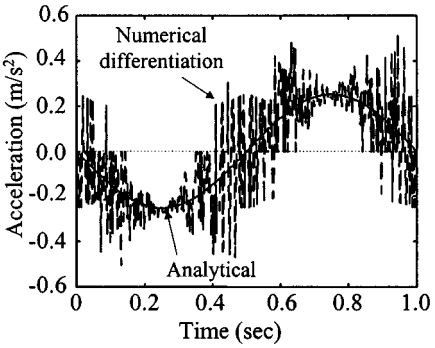

Fig. 5. Analytic and numerical differentiation based accelerations for sinewave velocity profile with amplitude of 0.04 m/s and frequency of 1 Hz.

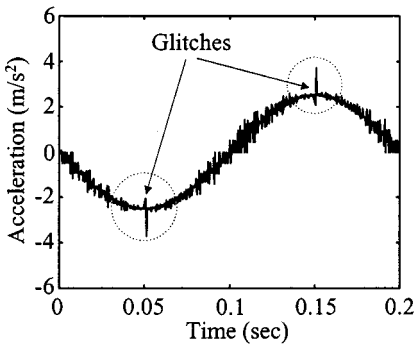

Fig. 6. Analytic and numerical differentiation based accelerations for sinewave velocity profile with amplitude of 0.04 m/s and frequency of 5 Hz.

a circular motion is realized by two sinusoidal profiles applied to two perpendicular axes in real applications. The reference acceleration a_r can then be given by

$$a_r = -V\omega\sin(\omega t). \tag{4}$$

A large error in acceleration estimation occurs frequently around zero acceleration regions where the change in velocity is very small. This phenomenon can be analyzed as follows. The sampling period T_s in Fig. 1 is 400 μs, and the period of the auxiliary pulse is set to 1 μs, as mentioned before. Hence, the denominator of (2), $T_v = T_s + \Delta T$, has a maximum error of ± 1 μs. Since this corresponds to an error of $\pm 0.25\%$ ($=\pm 1/400$) with respect to T_s ($=400$ μs), the velocity value based the M/T method has the same amount of error. Assume that two consecutive velocities v_1 and v_2 are obtained by the M/T method. Since each velocity may have an error of $\pm 0.25\%$, the velocity change Δv $(=v_2 - v_1)$ may have a maximum error of $\pm 0.5\% \times v_r$. The reference acceleration is the derivative of v_r, but can also be expressed by numerical differentiation as follows:

$$a = \frac{\Delta v}{T_v} \approx \frac{\Delta v}{T_s}. \tag{5}$$

Note that $T_v \approx T_s$ holds in Fig. 4, since the velocity reaches the amplitude V at the zero acceleration of $a_r = 0$. Substitution of (3) and (4) into (5) yields

$$\frac{\Delta v}{v_r} = -T_s\omega\tan(\omega t). \tag{6}$$

The left-hand side of (6) represents the ratio of velocity change to the velocity at the time when the acceleration is determined. Since Δv may contain an error as much as $\pm 0.5\% \times v_r$, the right-hand side of (6) lies within the error bound of the velocity measurement when $\Delta v/v_r < 0.5\%$, and thus the acceleration value computed by (5) in this case is meaningless. As the product of T_s and ω becomes larger, the region for $T_s\omega\tan(\omega t) > 0.5\%$, also grows and thus the range in which (6) is valid increases. Since T_s is usually predetermined in a control system, the valid range for acceleration computation grows as the frequency of a velocity signal increases.

Now, the above analysis will be investigated by actual acceleration detection. Fig.5 shows the acceleration estimated by numerical differentiation for the sinewave velocity profile with the amplitude of 0.04 m/s and the frequency of $\omega = 1$ Hz. When compared with the reference acceleration computed by (4), the acceleration estimate by numerical difference based shows severe variation, especially around the zero acceleration. Fig. 6 shows the result with the increased frequency of $\omega = 5$ Hz,

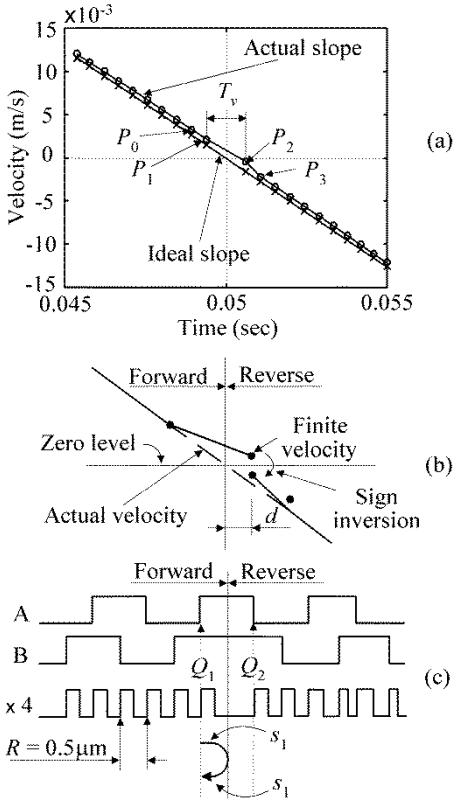

Fig. 7. Velocity detection around zero velocity by M/T method.

where variations in the acceleration signal significantly reduce, but it can be seen that it is still difficult to obtain accurate acceleration values around the zero acceleration region.

On the other hand, it is observed that the abnormal glitch signals appear in the acceleration signal around the zero velocity region. Since the velocity profile of (3) is applied, such an abnormal signal is not possible. Fig. 7(a) shows the enlarged portion of the low-velocity region (i.e., around 0.05 s in Fig. 6). The M/T-based velocity estimation is not able to detect zero velocity accurately and generates a discontinuity from the positive to negative velocity value. This is because the M/T method requires at least one pulse to determine the velocity, thus leading to mR of (2)'s being always positive. That is, zero velocity detection is inherently impossible with the M/T method. As shown in Fig. 7(b), the finite velocity value is computed after the motor passes the zero velocity point at which the direction of the motor changes and advances d, since the period T_v becomes maximum

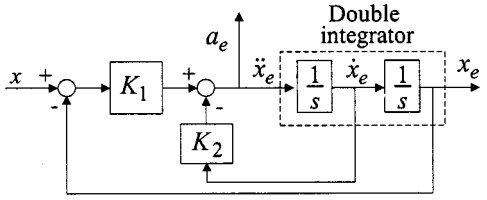

Fig. 8. Block diagram of low-acceleration estimator.

around the zero velocity region in the M/T method. Note that at this point, the sign of the velocity becomes negative, since the direction already has been reversed.

The same situation can be explained in terms of the encoder pulse output as follows. The rising edge of the pulse is detected at the position Q_1 of Fig. 7(c) during the forward movement, and then the rising edge is again detected at Q_2 during the reverse movement after the direction change. The positions Q_1 and Q_2 are physically identical, since the motor moves s_1 in the forward direction and then moves back s_1 in the reverse direction. Thus, the velocity must be zero because no displacement occurs during that period. In the actual velocity computation, however, one pulse of $R = 0.5\,\mu$m is counted and Q_2 is considered as negative, thus resulting in the negative velocity at P_2. That is, an abnormal velocity is detected between P_1 and P_2, and the acceleration estimate using this velocity value causes the glitch signal in Fig. 6.

In summary, the acceleration estimation based on numerical differentiation may be very inaccurate in both the low-acceleration and low-velocity regions. Therefore, some new approach to resolve this problem is required.

III. Low-Acceleration Estimator

A. Structure of a Low-Acceleration Estimator

In general, velocity is obtained by differentiating displacement and acceleration by differentiating velocity, or

$$a = \frac{d}{dt}v = \frac{d}{dt}\left(\frac{dx}{dt}\right) \tag{7}$$

where a, v, and x are the acceleration, velocity, and displacement, respectively. Based on this basic relation, a low-acceleration estimator, which is especially useful for low-acceleration and low-velocity ranges, is proposed in this paper. This estimator is based on the following two facts.

1) The displacement information from the encoder signal is very accurate.
2) Numerical integration provides more stable and accurate results than numerical differentiation.

Fig. 8 shows the structure of a low-acceleration estimator, which includes a double integrator. The acceleration estimate a_e is computed from the displacement x measured from the encoder, the estimated displacement x_e from the double integrator, and the estimated velocity v_e $(=dx_e/dt)$. That is, the PD control in the form of

$$a_e = K_1(x - x_e) - K_2\frac{dx_e}{dt} \tag{8}$$

is performed so that the estimated displacement x_e follows the actual displacement x. Based on (8), the transfer function from x to x_e in the block diagram of Fig. 8 can be obtained by

$$\frac{x_e}{x} = \frac{K_1}{s^2 + K_2 s + K_1} = \frac{\omega_b^2}{s^2 + 2\zeta\omega_b s + \omega_b^2} \tag{9}$$

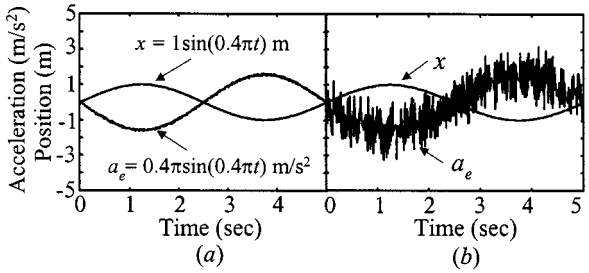

Fig. 9. Estimated acceleration responses of the PD controller: (a) excluding dx/dt in the derivative term and (b) including dx/dt in the derivative term.

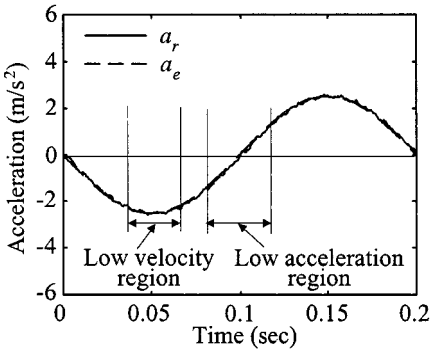

Fig. 10. Analytic and LAE-based accelerations for sinewave velocity profile with amplitude of 0.04 m/s and frequency of 5 Hz.

where ω_b represents the bandwidth of the low-acceleration estimator. The gains K_1 and K_2 of the PD controller are readily determined from the required bandwidth of the estimator.

Note that the actual displacement x is not included in the derivative term in (8). As shown in Fig. 9, the acceleration response without dx/dt in the derivative action [Fig. 9(a)] is much better than that with dx/dt included [Fig. 9(b)]. This can be explained as follows. The displacement signal x from the encoder contains not only the low-frequency displacement information but also high-frequency components caused by the discontinuity of the pulse signal, since x can take on the integer multiple of the encoder resolution (0.5 μm in this case). Thus, the differentiation of x may cause severe noise, leading to the inaccurate acceleration estimate. Another minor reason is that the transfer function has the standard form as in (8) with dx/dt excluded, which enables the gains K_1 and K_2 to be determined easily.

The proposed estimator is not hardware, but just a computer algorithm implemented in discrete-time form. The double integrator is represented in digital form by

$$\begin{Bmatrix} x_{e1}(k+1) \\ x_{e2}(k+1) \end{Bmatrix} = \begin{bmatrix} 0 & T_s \\ 0 & 0 \end{bmatrix} \begin{Bmatrix} x_{e1}(k) \\ x_{e2}(k) \end{Bmatrix} + \begin{Bmatrix} T_s^2 \\ T_s \end{Bmatrix} a_e(k) \tag{10}$$

where the state variables x_{e1}, x_{e2}, and a_e represent the estimated displacement, velocity, and acceleration, respectively, and T_s is the sampling period. The digital PD controller with discretized gains K_{D1}, K_{D2} corresponding to (8) is given by

$$a_e(k) = K_{D1}[x(k) - x_{e1}(k)] - K_{D2}x_{e2}(k). \tag{11}$$

Fig. 10 shows the acceleration response obtained by the low-acceleration estimator in the same condition as in Fig. 5. It is observed that the poor responses in Figs. 5 and 6 around the low-acceleration and low-velocity regions were much improved

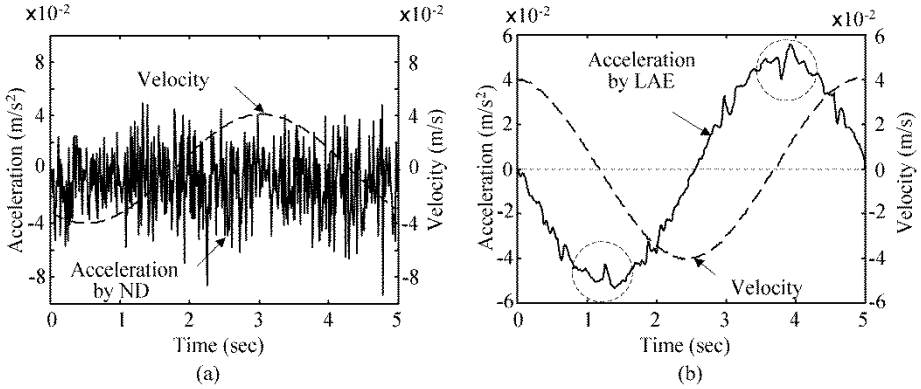

Fig. 11. Acceleration responses: (a) based on ND and (b) based on LAE.

in Fig. 10. In Fig. 11, the linear motor was controlled to follow the reference sinusoidal velocity profile with very low frequency of 0.2 Hz, and the response by the low-acceleration estimator was compared with that by numerical differentiation. It is noticed in Fig. 11(a) that accurate sensing of the acceleration is almost impossible in the entire region, not to mention the region with direction reversal. However, the proposed acceleration estimator can determine acceleration with relative accuracy in the entire region. At the zero velocity region, some variations in acceleration are observed, because a temporary stop region arises due to friction existing in the linear motor at direction reversal.

One of the important design considerations of the low-acceleration estimator is its damping ratio ζ and bandwidth ω_b. The damping ratio is usually selected as 0.707, which corresponds to the critical damping, because it provides the fastest response without overshoot. On the other hand, it is difficult to give a general guideline for the determination of the bandwidth, since it is dependent upon the situations. However, the experimental results in Fig. 12 showing the acceleration estimates with the bandwidths of 50 and 150 Hz for each damping ratio ζ of 0.707 may be a good guideline for the bandwidth determination. Although the tracking capability of the estimator generally improves as the bandwidth becomes larger, the large bandwidth can adversely affect the estimation performance, as observed in Fig. 12(b). Since the actual displacement is in the form of a step function, the large bandwidth enables the estimator to follow the discontinuity portion of x, which is characterized by high-frequency components. However, the response is still better than that in Fig. 5 in which numerical differentiation is employed. Note that the bandwidth of the low-acceleration estimator does not need to be large if the variation in the acceleration under consideration is not very large.

B. Combined Acceleration Estimator

The acceleration estimation based on numerical differentiation can provide very useful and accurate results on the condition that the velocity signals have relatively large variations and keep off of the low-velocity region. However, velocity signals are not alterable once they are generated, and low-velocity situations frequently occur due to direction reversal or the stick-slip phenomenon. As shown before, the proposed low-acceleration estimator can function well in such unavoidable situations.

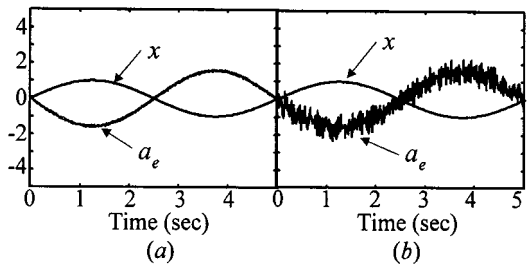

Fig. 12. Estimated acceleration responses for different bandwidths: (a) $\omega_b = 50$ Hz, $\zeta = 0.707$ and (b) $\omega_b = 150$ Hz, $\zeta = 0.707$.

It is desirable to perform acceleration estimation by combining the proposed low-acceleration estimator and numerical differentiation. For this purpose, the following criteria are employed.

Condition 1) The velocity v is smaller than the specified velocity $v_{\min}$.

Condition 2) The ratio of velocity change to velocity $\Delta v/v$ is smaller than the specified value C.

Note that Conditions 1) and 2) represent the criteria for a zero velocity region and a zero acceleration region, respectively. The procedure is as follows. First, v and $\Delta v/v$ are computed by the M/T method. Then, if either of the conditions is met, the low-acceleration estimator is used; otherwise, the acceleration is estimated by numerical differentiation.

The value $v_{\min}$ of Condition 1) can be determined as the velocity corresponding to one encoder pulse per sampling period T_s, because the velocity smaller than this may cause the velocity updating period T_v to become excessively large. The value $C\ (=\Delta v/v)$ of Condition 2) can be set to 5% according to the argument associated with (6). Although the numerical differentiation begins to give useful data for the velocity region of $\Delta v/v_r > 0.5\%$ from the discussion in Section II-C, the region in which the numerical differentiation provides accurate results may be selected as $\Delta v/v_r > 5\%$ from the practical point of view.

To investigate the validity of this approach, a simulation as in Fig. 13 was performed. Consider the arbitrary velocity signal with a wide range of frequency components given by

$$v_r = 0.08\sin(2\pi t) + 0.16\exp[-100(t-0.5)^2] \times \sin(20\pi t + 1). \quad (12)$$

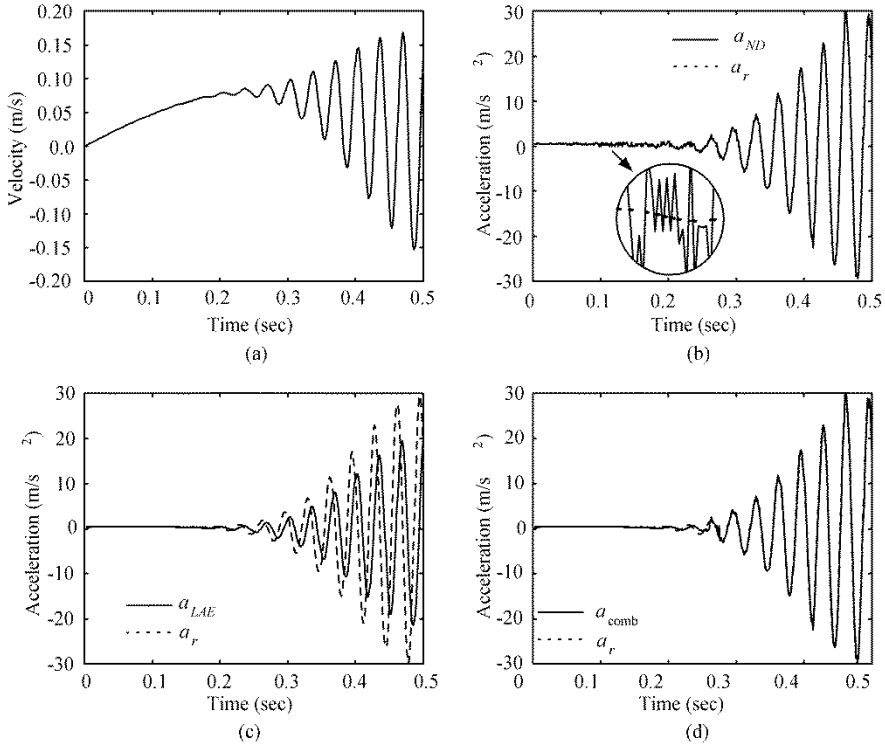

Fig. 13. Estimated accelerations of various estimation methods: (a) velocity profile, (b) acceleration by ND, (c) acceleration by LAE with $\omega_b = 50$ Hz, $\zeta = 0.707$, and (d) acceleration by a combination of ND and LAE ($V_{\min} = 0.0012$ m/s, $C = 0.05$).

The exponential term of (12) was used as a weighting factor, which yields the high-frequency components around 0.5 s. Note that the analytical expression for the velocity is used since its derivative provides an accurate reference acceleration a_r, which can be compared with the actual acceleration estimates. The acceleration response based on numerical differentiation as shown in Fig. 13(b) provides inaccurate results in the low-acceleration region, while that based on the low-acceleration estimator as shown in Fig. 13(c) yields poor results in the high-acceleration region. However, Fig. 13(d) with suitable switching between the two approaches shows good acceleration response over a wide range of velocity.

IV. Friction Compensation Using Low-Acceleration Estimator

In friction compensation control systems, friction observers are used to estimate the friction force [7]–[9], and the main purpose of the friction observer is to detect changes in acceleration due to friction. Its use is important because external forces such as friction force cause immediate variation in acceleration. In order to construct an accurate acceleration observer, plant parameters, such as motor inertia and load inertia, are needed, but they tend to vary depending on the task being performed, which makes construction of the observer difficult. Since friction compensation is usually performed in the low-velocity region, the proposed low-acceleration estimator can serve as a useful tool in this situation. Fig.14 shows the block diagram of a friction compensation system, which is composed of the proportional integral (PI) controller and the low-acceleration estimator. The control signal sent to the motor in this system is given by

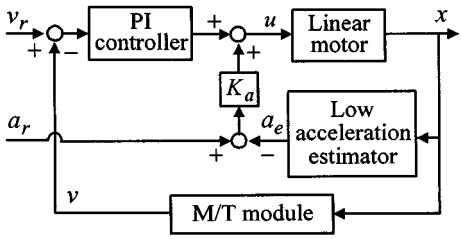

Fig. 14. PI velocity control system with LAE.

$$u = K_P(v_r - v) + K_I \int (v_r - v)\,dt + K_a(a_r - a_e) \quad (13)$$

where

u	control signal;
K_P, K_I, K_a	proportional gain, integral gain, and gain for acceleration compensation, respectively.
v_r, v, a_r	reference velocity, actual velocity, and reference acceleration, respectively;
a_e	estimated acceleration from the low-acceleration estimator.

Note that the reference velocity and acceleration are predetermined since the XY table of a machine tool follows the predetermined path. The third term in (13) is added in order to expedite the friction compensation using the error between the reference acceleration a_r and estimated acceleration a_e.

Fig.15 shows the experimental results representing the velocity tracking performance of the proposed friction compen-

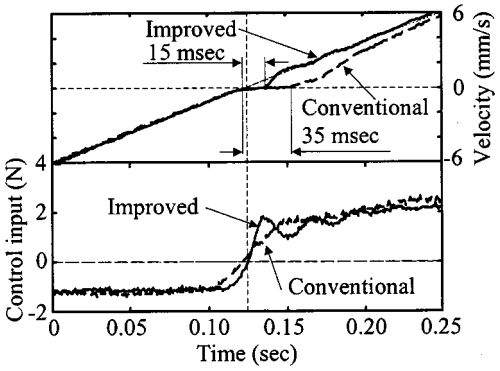

Fig. 15. Velocity responses and control signals for conventional PI controller (dashed) with proportional gain $K_P = 60$, integral gain, $K_I = 2000$, and friction compensation controller with LAE (solid) with acceleration gain $K_a = 25$ (Vs^2/m), where V is volt.

sation system. Compared to the result of where the PI controller without friction compensation is applied, it is observed that the stop region of the moving part of the motor has been reduced significantly from 35 to 15 ms. Furthermore, the response faithfully follows the reference velocity immediately after the end of the stop region. Consider the control signal sent to the motor in Fig. 15. In the case of the PI controller without friction compensation, the control signal gradually increases after the conversion of the direction by the integral action. On the other hand, with the aid of friction compensation, the control signal quickly increases thanks to the control input caused by the difference between the estimated and reference accelerations.

V. Conclusion

In this paper, it was analytically shown that the acceleration estimated by numerical differentiation yields inaccurate results in the low-velocity and low-acceleration regions. To overcome this inaccuracy, the low-acceleration estimator was proposed to provide accurate acceleration estimates, especially in the low-velocity and low-acceleration regions. Since this algorithm is based on numerical integration, the bandwidth of the low-acceleration estimator is rather limited. Therefore, this estimator can be used in combination with the traditional numerical differentiation, which is quite useful except for low-velocity or low-acceleration regions. It was shown in various simulations and experiments that this combined acceleration estimator can yield accurate acceleration estimates over a wide range of velocities.

The proposed low acceleration estimator was applied to friction compensation control systems in order to verify its validity. With this estimator, the stop region of the motor was clearly estimated, which is caused by friction in the low-velocity region. Furthermore, the effects of low-velocity friction, especially at the direction reversal, can be significantly reduced in the friction compensation control system, which is attributed to the accurate sensing of the zero acceleration by the proposed estimator.

References

[1] R. H. Brown, S. C. Schneider, and M. G. Mulligan, "Analysis of algorithms for velocity estimation from discrete position versus time data," *IEEE Trans. Ind. Electron.*, vol. 39, pp. 11–19, Feb. 1992.

[2] T. Ohmae, T. Matsuda, and K. Kamiyama, "A microprocessor-controlled high-accuracy wide-range speed regulator for motor drives," *IEEE Trans. Ind. Electron.*, vol. IE-29, pp. 207–211, Aug. 1982.

[3] H. W. Kim, J. W. Choi, and S. K. Sul, "Accurate position control for AC servo motor using novel speed estimator," in *Proc. IEEE Int. Conf. Industrial Electronics, Control, and Instrumentation*, 1995, pp. 627–632.

[4] P. R. Belanger, P. Dobrovolny, A. Helmy, and X. Zhang, "Estimation of angular velocity and acceleration from shaft-encoder measurements," *Int. J. Robot. Res.*, vol. 17, no. 11, pp. 1225–1233, Nov. 1998.

[5] A. Dunworth, "Digital instrumentation for angular velocity and acceleration," *IEEE Trans. Instrum. Meas.*, vol. IM-18, pp. 132–138, June 1969.

[6] S. Nicosia and P. Tomei, "Robot control by using only joint position measurements," *IEEE Trans. Automat. Contr.*, vol. 9, pp. 1058–1061, Sept. 1990.

[7] M. Iwasaki and N. Matsui, "Observer-based nonlinear friction compensation in servo drive system," in *Proc. 4th Int. Workshop Advanced Motion Control*, 1996, pp. 344–348.

[8] M. Iwasaki, T. Shibata, and N. Matsui, "Disturbance-observer-based nonlinear friction compensation in table drive system," *IEEE/ASME Trans. Mechatron.*, vol. 4, pp. 3–8, Mar. 1999.

[9] J. Ishikawa and M. Tomizuka, "Pivot friction compensation using an accelerometer and a disturbance observer for hard disk drives," *IEEE/ASME Trans. Mechatron.*, vol. 3, pp. 194–201, Sept. 1998.

Se-Han Lee received the B.S. and M.S. degrees in mechanical engineering from Korea University, Seoul, in 1989 and 1991, respectively, where he is now pursuing the Ph.D. degree in the Department of Mechanical Engineering.

From 1991 to 1996, he was with Samsung Electronics Company. His current research interests include design and control of parallel manipulators and control of servo systems.

Jae-Bok Song received the B.S. and M.S. degrees in mechanical engineering from Seoul National University, Seoul, Korea, in 1983 and 1985, respectively, and the Ph.D. degree in mechanical engineering from the Massachusetts Institute of Technology (MIT), Cambridge, MA, in 1992.

From 1992 to 1993, he was a Research Associate at MIT. He joined the Faculty of the Department of Mechanical Engineering, Korea University, Seoul, in 1993, where he has been an Associate Professor since 1997. His current research interests include design of haptic devices, mechanism design, control and navigation of omnidirectional mobile robots, and design and control of parallel manipulators.